J|A|C|S ARTICLES

Published on Web 12/11/2008

Surface Functionalization of Nanomaterials with Dendritic Groups: Toward Enhanced Binding to Biological Targets

Amanda L. Martin,[†] Bo Li,[†] and Elizabeth R. Gillies*[,†,‡]

Department of Chemistry and Department of Chemical and Biochemical Engineering, The University of Western Ontario, 1151 Richmond Street, London, Ontario N6A 5B7, Canada

Received September 11, 2008; E-mail: egillie@uwo.ca

Abstract: A diverse array of nanomaterials ranging from polymer assemblies to nanoparticles has been under development for biomedical applications in recent years. A key aspect of these applications is the ability to target the materials to the desired locations in vivo by exploiting their size or through the conjugation of active targeting groups. While nanoscale scaffolds may provide advantages such as the multivalent presentation of targeting ligands, the binding of these ligands may also be inhibited by interfering polymer chains at their surfaces. This aspect was investigated here by preparing poly(butadiene-*block*-ethylene oxide) vesicles and dextran-coated iron oxide nanoparticles functionalized with dendritic and nondendritic displays of mannose, a well-known multivalent ligand. The binding of these systems to the mannose-binding protein Concanavalin A was compared using a hemagglutination assay. It was found that the dendritic systems exhibited 1−2 orders of magnitude enhancement in binding affinity relative to the nondendritic displays. This result is attributed to the ability of the dendritic groups to overcome steric inhibition by polymer chains at the material surface and also to the presentation of ligands in localized clusters. It is anticipated that these results should be applicable to a wide range of nanomaterials with polymers at their surfaces and that the method by which biological ligands are conjugated to the surfaces of nanoparticles and polymer assemblies should be carefully considered.

Introduction

In the past years, a tremendous number of new nanomaterials have been developed for biomedical applications. Water-soluble linear and dendritic polymer architectures have been used for both drug delivery and diagnostics through the conjugation of drugs and contrast agents,[1,2] while hydrophobic polymers have been used to prepare nanoparticles that can noncovalently encapsulate these agents.[3,4] Amphiphilic polymers have been shown to assemble into supramolecular structures ranging from micelles[5] to wormlike assemblies[6] and vesicles,[7] and these structures are capable of encapsulating bioactive molecules into their hydrophilic or hydrophobic compartments. Inorganic nanomaterials such as superparamagnetic iron oxide nanoparticles[8,9] and quantum dots[10] with biocompatible polymer coatings are also of significant interest in imaging applications.

For most nanomaterials aimed at biomedical applications, the first significant challenge is to avoid undesirable uptake by the reticuloendothelial system. This can often be accomplished by the conjugation of polymers such as poly(ethylene oxide),[11,12] while limiting the size of the materials to below ∼150 nm has also been found to be important.[13] The next step is to achieve selective targeting of the system to the site of interest in vivo, such that drugs or contrast agents provide increased efficacy or sensitivity respectively. In some cases, this can be accomplished passively via the enhanced permeation and retention (EPR) effect, which allows for the selective accumulation of nanosized systems relative to small molecules in tumors due to their "leaky" vasculature.[14] An alternative approach involves the conjugation of active targeting groups. For example, the antibody herceptin has been used to target nanoparticles to tumors expressing the Her/neu2 receptor,[15,16] while peptides containing the arginine−glycine−phenylalanine (RGD) motif

[†] Department of Chemistry.
[‡] Department of Chemical and Biochemical Engineering.

(1) Lee, C. C.; MacKay, J. A.; Fréchet, J. M. J.; Szoka, F. C. *Nat. Biotechnol.* **2005**, *23*, 1517–1526.
(2) Duncan, R. *Nat. Rev. Drug Discovery* **2003**, *2*, 347–360.
(3) Soppimath, K. S.; Aminabhavi, T. M.; Kulkarni, A. R.; Rudzinski, W. E. *J. Controlled Release* **2001**, *70*, 1–20.
(4) Vasir, J. K.; Labhasetwar, V. *Adv. Drug Delivery Rev.* **2007**, *59*, 718–728.
(5) Kataoka, K.; Harada, A.; Nagasaki, Y. *Adv. Drug Delivery Rev.* **2001**, *47*, 113–131.
(6) Dalhaimer, P.; Engler, A. J.; Parthasarathy, R.; Discher, D. E. *Biomacromolecules* **2004**, *5*, 1714–1719.
(7) Discher, D. E.; Eisenberg, A. *Science* **2002**, *297*, 967–973.
(8) Corot, C.; Robert, P.; Idée, J. M.; Port, M. *Adv. Drug Delivery Rev.* **2006**, *58*, 1471–1504.
(9) Laurent, S.; Forge, D.; Port, M.; Roch, A.; Robic, C.; Vander Elst, L.; Muller, R. N. *Chem. Rev.* **2008**, *108*, 2064–2110.
(10) Gao, X.; Yang, L.; Petros, J. A.; Marshall, F. F.; Simons, J. W.; Nie, S. *Curr. Opin. Biotechnol.* **2005**, *16*, 63–72.
(11) Gref, R.; Domb, P.; Quellec, T.; Blunk, T.; Muller, R. H.; Verbavatz, J. M.; Langer, R. *Adv. Drug Delivery Rev.* **1995**, *16*, 215–233.
(12) Gillies, E. R.; Dy, E.; Fréchet, J. M. J.; Szoka, F. C. *Mol. Pharmaceutics* **2005**, *2*, 129–138.
(13) Gaumet, M.; Vargas, A.; Gurny, R.; Delie, F. *Eur. J. Pharm. Biopharm.* **2008**, *69*, 1–9.
(14) Maeda, H.; Wu, J.; Sawa, T.; Matsumura, Y.; Hori, K. *J. Controlled Release* **2000**, *65*, 271–284.
(15) Huh, Y. M.; Jun, Y. W.; Song, H. T.; Kim, S.; Choi, J. S.; Lee, J. H.; Yoon, S.; Kim, K. S.; Shin, J. S.; Suh, J. S.; Cheon, J. *J. Am. Chem. Soc.* **2005**, *127*, 12387–12391.
(16) Lee, J. H.; Huh, Y. M.; Jun, Y. W.; Seo, J. W.; Jang, J. T.; Song, H. T.; Kim, S.; Cho, E. J.; Yoon, H. G.; Suh, J. S.; Cheon, J. *Nat. Med.* **2007**, *13*, 95–99.

10.1021/ja807220u CCC: $40.75

have been used to target nanoparticles,[17−19] and micelles[20,21] to tumors expressing elevated levels of the $\alpha_v\beta_3$ integrins.

Small-molecule targeting groups are also particularly attractive due to their ease of preparation and simple conjugation chemistry. Folic acid, a small molecule, has been extensively used for targeting dendritic polymers,[22,23] micelles,[24,25] and nanoparticles[26,27] to tumors expressing elevated levels of the folic acid receptor. Carbohydrates such as mannose and glucose have been demonstrated to provide enhanced delivery into macrophages[28,29] and bacteria.[30−32] Although small molecules often possess only moderate binding affinities for their biological targets, the incorporation of multiple copies of these molecules onto nanomaterial surfaces can provide multivalent systems which exhibit significantly enhanced binding.[33] On the other hand, some binding affinity may be lost through steric inhibition by polymer chains, which are present at the surface of most of these materials, and this effect has not yet been investigated in detail. In addition, the density and spatial distribution of ligands on the surfaces can also play a role. Thus, the goal of this work was to investigate whether the way in which biological ligands are displayed at the surfaces of polymer assemblies and nanoparticles affects their binding to biological targets.

As illustrated in Figure 1, it was anticipated that the introduction of ligands to surfaces using a dendritic approach would provide enhanced availability of the ligands, in comparison with individual small molecules conjugated without a dendritic scaffold, which may become easily buried within a polymer layer at the surface. For this study, mannose was selected as a model biological ligand, as its multivalent binding to targets such as Concanavalin A (Con A) has been extensively investigated and a number of assays have been developed to evaluate this binding.[34−38] Dendritic displays of mannose have been previously demonstrated by several groups to provide enhanced binding to Con A in comparison with monovalent mannose,[39−41] but their effect on the presentation of mannose at polymeric surfaces has not been investigated. Here, the effect of dendritic versus nondendritic surface functionalization was investigated using polymer vesicles formed from poly(butadiene-*block*-ethylene oxide) (PBD-PEO) and dextran-coated iron oxide nanoparticles as model materials. The results described here are expected to be generalizable to a wide variety of materials, thus providing a framework for enhancing targeting efficiency for a wide range of biomedical applications.

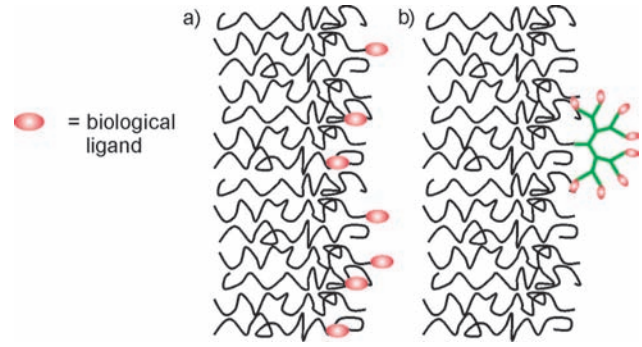

Figure 1. Schematic comparison of a surface functionalized with (a) nondendritic versus (b) dendritic groups.

Results and Discussion

Preparation of Polymer Vesicles Functionalized with Dendritic Mannose. Polymer vesicles are among the classes of polymer assemblies that have received significant attention in recent years.[42−46] The availability of both hydrophobic and hydrophilic compartments, as well as their increased strength and stability relative to their phospholipid vesicle analogues (liposomes), have made them attractive materials for recent applications in imaging and drug delivery.[47−53] Thus, they are ideal materials for the exploration of surface functionalization

(17) Zhang, N.; Chittasupho, C.; Duangrat, C.; Siahaan, T. J.; Berkland, C. *Bioconjugate Chem.* **2008**, *19*, 145–152.
(18) Montet, X.; Montet-Abou, K.; Reynolds, F.; Weissleder, R.; Josephson, L. *Neoplasia* **2006**, *8*, 214–222.
(19) Lee, H.; Li, Z.; Chen, K.; Hsu, A. R.; Xu, C.; Xie, J.; Sun, S.; Chen, X. *J. Nucl. Med.* **2008**, *49*, 1371–1379.
(20) Oba, M.; Fukushima, S.; Kanayama, N.; Aoyagi, K.; Nishiyama, N.; Koyama, H.; Kataoka, K. *Bioconjugate Chem.* **2007**, *18*, 1415–1423.
(21) Nasongkla, N.; Shuai, X.; Ai, H.; Weinberg, B. D.; Pink, J.; Boothman, D. A.; Gao, J. *Angew. Chem., Int. Ed.* **2004**, *43*, 6323–6327.
(22) Konda, S. D.; Wang, S.; Brechbiel, M.; Wiener, E. C. *Invest. Radiol.* **2002**, *37*, 199–204.
(23) Quintana, A.; Raczka, E.; Piehler, L.; Lee, I.; Mye, A.; Majoros, I.; Patri, A.; Thomas, T.; Mulé, J.; Baker, J. R. J. *Pharm. Res.* **2002**, *19*, 1310–1316.
(24) Bae, Y.; Nishiyama, N.; Kataoka, K. *Bioconjugate Chem.* **2007**, *18*, 1131–1139.
(25) Lee, E. S.; Na, K.; Bae, Y. H. *J. Controlled Release* **2005**, *103*, 405–418.
(26) Stella, B.; Arpicco, S.; Peracchia, M. T.; Desmaele, D.; Hoebeke, J.; Renoir, M.; D'Angelo, J.; Cattel, L.; Couvreur, P. *J. Pharm. Sci.* **2000**, *89*, 1452–1464.
(27) Nayak, S.; Lee, H.; Chmielewski, J.; Lyon, L. A. *J. Am. Chem. Soc.* **2004**, *126*, 10258–10259.
(28) Jiang, H.; Kang, M. L.; Quan, J.; Kang, S. G.; Akaike, T.; Yoo, H. S.; Cho, C. *Biomaterials* **2008**, *29*, 1931–1939.
(29) Zarabi, B.; Nan, A.; Zhuo, J.; Gullapalli, R.; Ghandehari, H. *Mol. Pharmaceutics* **2006**, *3*, 550–557.
(30) Joralemon, M. J.; Murthy, K. S.; Remsen, E. E.; Becker, M. L.; Wooley, K. L. *Biomacromolecules* **2004**, *5*, 903–913.
(31) Pasparakis, G.; Alexander, C. *Angew. Chem., Int. Ed.* **2008**, *47*, 4847–4850.
(32) Kim, B. S.; Yang, W. Y.; Ryu, J. H.; Yoo, Y. S.; Lee, M. *Chem. Commun.* **2005**, 2035–2037.
(33) Mammen, M.; Choi, S. K.; Whitesides, G. M. *Angew. Chem., Int. Ed.* **1998**, *37*, 2754–2794.
(34) Williams, B. A.; Chervenek, M. C.; Toone, E. J. *J. Biol. Chem.* **1992**, *267*, 22907–22911.
(35) Bittiger, H.; Schnebli, H. P., Eds.; *Concanavalin A as a Tool*; John Wiley and Sons, Ltd.: New York, 1976.
(36) Kanai, M.; Mortell, K. H.; Kiessling, L. L. *J. Am. Chem. Soc.* **1997**, *119*, 9931–9932.
(37) Gestwicki, J. E.; Cairo, C. W.; Strong, L. E.; Oetjen, K. A.; Kiessling, L. L. *J. Am. Chem. Soc.* **2002**, *124*, 14922–14933.
(38) Roy, R. *Curr. Opin. Struct. Biol.* **1996**, *6*, 692–702.
(39) Wu, P.; Malkoch, M.; Hunt, J. N.; Vestberg, R.; Kaltgrad, E.; Finn, M. G.; Fokin, V. V.; Sharpless, K. B.; Hawker, C. J. *Chem. Commun.* **2005**, 5775–5777.
(40) Branderhorst, H. M.; Ruijtenbeek, R.; Liskamp, R. M. J.; Pieters, R. J. *ChemBioChem* **2008**, *9*, 1836–1844.
(41) Woller, E. K.; Cloninger, M. J. *Org. Lett.* **2002**, *4*, 7–10.
(42) Zhang, L.; Eisenberg, A. *Science* **1995**, *268*, 1728–1731.
(43) Discher, B. M.; Won, Y. Y.; Ege, D. S.; Lee, J. C. M.; Bates, F. S.; Discher, D. E.; Hammer, D. A. *Science* **1999**, *284*, 1143–1145.
(44) Checot, F.; Lecommandoux, S.; Gnanou, Y.; Klok, H. A. *Angew. Chem., Int. Ed.* **2002**, *41*, 1339–1343.
(45) Morishima, Y. *Angew. Chem., Int. Ed.* **2007**, *46*, 1370–1372.
(46) Cornelissen, J. J. L. M.; Fischer, M.; Sommerdijk, N. A. J. M.; Nolte, R. J. M. *Science* **1998**, *280*, 1427–1430.
(47) Cheng, Z.; Tsourkas, A. *Langmuir* **2008**, *24*, 8169–8173.
(48) Broz, P.; Ben-Haim, N.; Grzelakowski, M.; Marsch, S.; Meier, W.; Hunziker, P. *J. Cardiovasc. Pharmacol.* **2008**, *51*, 246–252.
(49) Lomas, H.; Canton, I.; MacNeil, S.; Du, J.; Armes, S. P.; Ryan, A. J.; Lewis, A. L.; Battaglia, G. *Adv. Mater.* **2007**, *19*, 4238–4243.
(50) Rameez, S.; Alosta, H.; Palmer, A. F. *Bioconjugate Chem.* **2008**, *19*, 1025–1032.
(51) Ranquin, A.; Versées, W.; Meier, W.; Steyaert, J.; van Gelder, P. *Nano Lett.* **2005**, *5*, 2220–2224.
(52) Ahmed, F.; Pakunlu, R. I.; Srinivas, G.; Brannan, A.; Bates, F.; Klein, M. L.; Minko, T.; Discher, D. E. *Mol. Pharmaceutics* **2006**, *3*, 340–350.

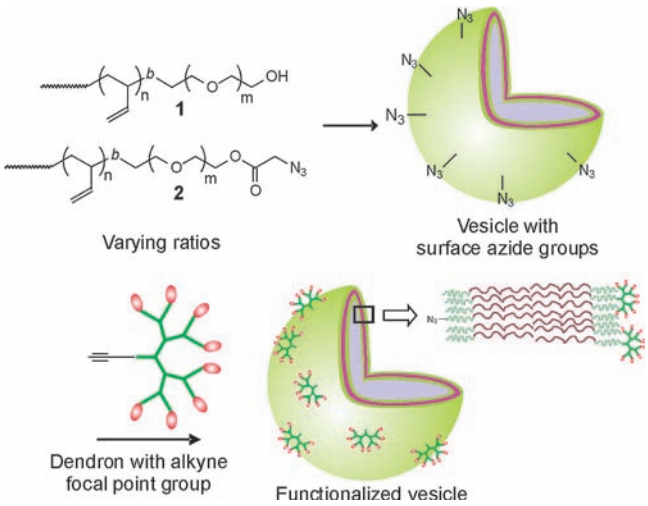

Figure 2. General approach for functionalization of vesicle surfaces with dendritic groups.

with dendritic and nondendritic ligands. Gillies and co-workers have recently reported a new approach for the functionalization of polymer vesicles with dendritic groups.[54] As illustrated in Figure 2, PBD-PEO having hydroxyl (**1**) or azide termini (**2**) can be mixed in varying ratios and assembled to form vesicles with controlled densities of surface azide groups. Dendrons with focal point alkynes can subsequently be conjugated to the surface azides providing controlled densities of dendritic groups on the vesicle surface. Therefore, the first step in this study was to prepare polymer vesicles functionalized with dendritic mannose using this approach.

To demonstrate that dendritic mannose could be conjugated to the polymer vesicle surface, dendron **3**[54] with peripheral amines and approximately one rhodamine molecule per dendron statistically was reacted with 2-isothiocyanato-α-D-mannopyranoside **4**[55] to provide dendron **5** as shown in Scheme 1. Incorporation of rhodamine into this dendron allowed the functionalized vesicles to be visualized by fluorescence confocal microscopy and also provided a means of quantifying the vesicle functionalization using ultraviolet−visible (UV−vis) spectroscopy as an extinction coefficient for dendron **5** could be measured. Due to the statistical nature of the dye functionalization, this dendron does not have a precise structure, but the presence of approximately one dye molecule and at least six mannose molecules on average per dendron was verified by NMR spectroscopy.

Vesicles having varying densities of azides were prepared by the hydration of polymer films containing the desired ratios of polymers **1** and **2**, followed by sonication (Figure 2). Dendron **5** was then conjugated to the surfaces of the vesicles using "click" cycloaddition conditions consisting of 1 mM $CuSO_4$, 25 mM sodium ascorbate, and 2.3 mM bathophenanthrolinedisulfonic acid to provide functionalized vesicles **6a**−**h** (Table 1). Excess dendron was removed by dialysis. Confocal fluorescence microscopy of the vesicles indicated that they were fluorescent, confirming the successful incorporation of the rhodamine functionalized dendron, and that a majority of the vesicles were

Scheme 1

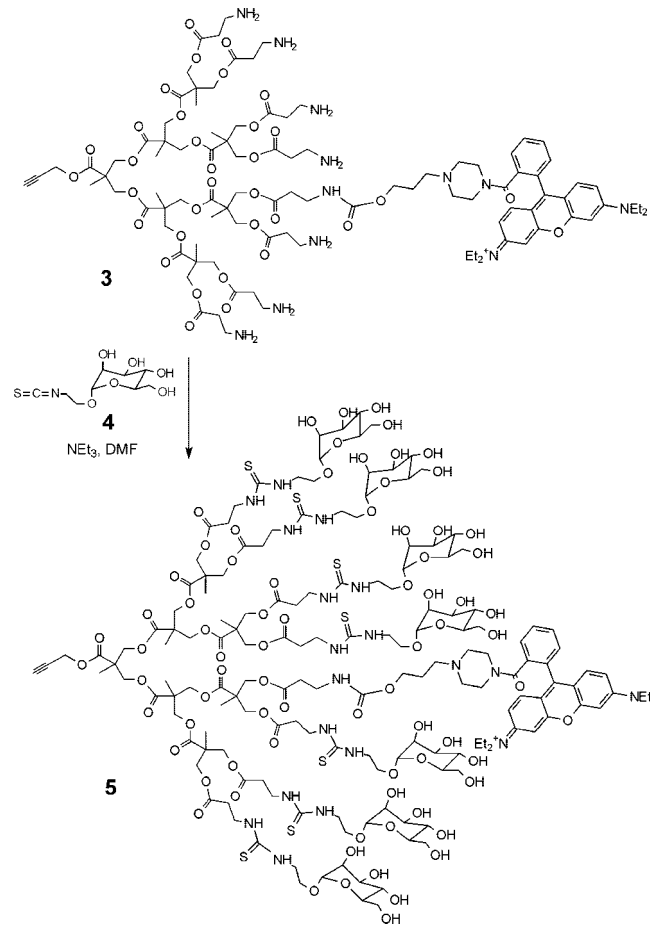

Table 1. Yields for the Functionalization of Polymer Vesicles Having Varying Densities of Surface Azide Groups with Dendron **5**

vesicles	% of PBD-PEO having terminal azide groups	% of PBD-PEO functionalized with dendron **5** (based on UV−vis)	% yield of conjugation
6a	0	none detected	NA
6b	5	3.4 ± 0.1	67 ± 2
6c	7	4.4	62
6d	10	4.4	44
6e	20	7.0	35
6f	40	10	25
6g	70	14	20
6h	100	21	21

single walled. At lower densities of azides on the vesicle surface, up to ∼40%, well-dispersed vesicles were observed following conjugation of the dendron (Figure 3a). At higher densities, including 70% and 100%, fluorescent aggregates were observed (Figure 3b). Similar aggregation was previously observed when dendron **3** was coupled to vesicles containing high percentages of surface azides,[54] and this aggregation has been attributed to vesicle destabilization due to the architecture of the resulting linear−dendritic polymers being unfavorable for vesicle formation when incorporated at high percentages. It is noteworthy that while the polymer vesicles investigated here were micrometer-sized for easy visualization by optical microscopy, it has been shown that the sizes of these PBD-PEO vesicles can be readily reduced to the nanometer range by extrusion.[56]

(53) Ghoroghchian, P. P.; Frail, P. R.; Susumu, K.; Blessington, D.; Brannan, A. K.; Bates, F. S.; Chance, B.; Hammer, D. A.; Therien, M. J. *Proc. Natl. Acad. Sci. U.S.A.* **2005**, *102*, 2922–2927.
(54) Li, B.; Martin, A.; Gillies, E. R. *Chem. Commun.* **2007**, 5217–5219.
(55) McBroom, C. R.; Samanen, C. H.; Goldstein, I. J. *Methods Enzymol.* **1972**, *28*, 212.
(56) Photos, P. J.; Bacakova, L.; Discher, B. M.; Bates, F. S.; Discher, D. E. *J. Controlled Release* **2003**, *90*, 323–334.

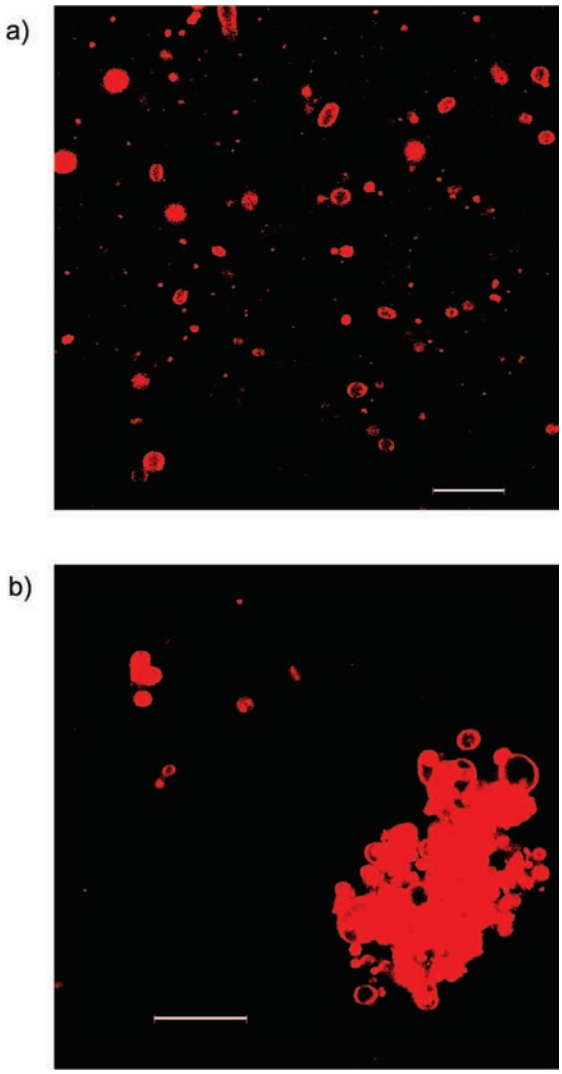

Figure 3. Confocal laser scanning microscopy images of polymer vesicles following conjugation of the fluorescent dendron **5**. (a) Well-dispersed vesicles resulted when low densities of surface azides were used (**6b**, 5%). (b) Aggregated vesicles resulted when high densities of surface azides were used (**6g**, 70%) (scale bar = 20 μm).

Following removal of water, the resulting mixture of polymers was taken up in DMF/MeOH (10:1) and the amount of conjugated dendron was quantified by UV−vis spectroscopy. As shown in Table 1, the functionalization yields were high at low azide densities but they rapidly dropped off at higher densities, presumably due to steric hindrance at the vesicle surface, which prevents further functionalization. It is noteworthy that yields of greater than 50% are considered high for this reaction, as close to half of the azides should reside on the interior of the vesicles are therefore not available for functionalization. At low azide densities, the yields in excess of 50% are attributed to the movement of some azide-functionalized polymers to the vesicle surface by various mechanisms during the 24 h reaction, followed by their functionalization. Similar yields were previously observed for the conjugation of dendron **3** to vesicles.[54] To ensure that the dialysis procedure for the removal of excess dendron was effective, the reaction was carried out on vesicles having no surface azide groups and no absorbance from the dendron was detected by UV−vis. In addition, to investigate the reproducibility of the functionalization procedure, the preparation of vesicle **6b** was carried out

Scheme 2

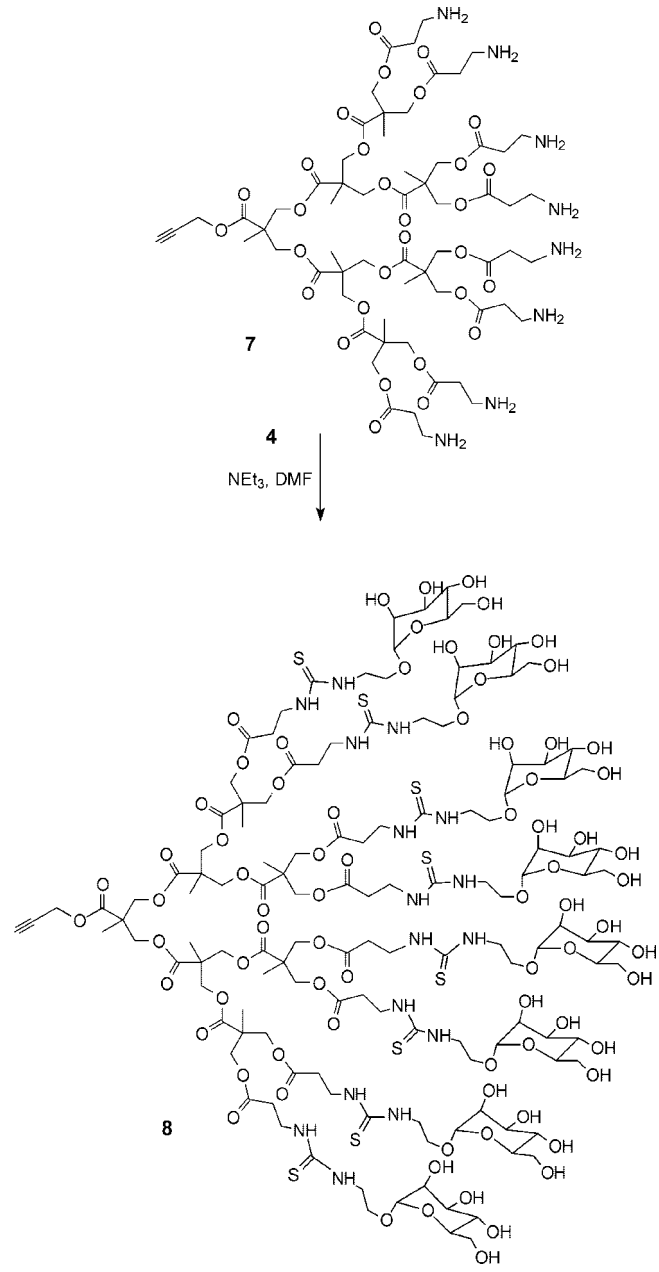

several times. The procedure was quite reproducible, providing a standard deviation of only 3%.

In order to investigate the binding of the dendritic mannose-functionalized vesicles to biological targets, it is desirable to avoid the incorporation of the rhodamine dye, which may sterically inhibit the mannose from binding. Therefore, as shown in Scheme 2, the amine-functionalized dendron **7**[54] was converted to dendron **8** having only mannose groups on its periphery. Characterization of dendron **8** was challenging due to broad peaks in the NMR spectrum, which can likely be attributed to intramolecular hydrogen bonding between the thiourea groups. Nevertheless, ^{1}H NMR integration indicated that there were at least seven mannose groups per dendron. The conjugation of this dendron to vesicles containing 5% surface azide groups was carried out as described above to provide dendritic mannose-functionalized vesicles **9** (Scheme 3). On the basis of the highly reproducible nature of the vesicle functionalization at this azide density and very modest difference

Scheme 3

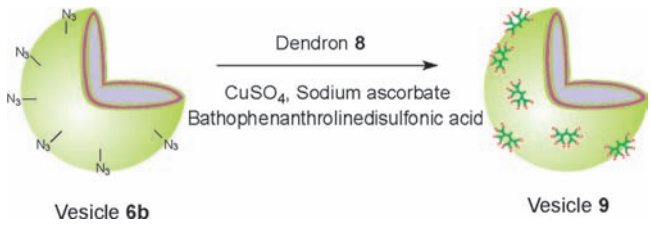

between dendrons **5** and **8**, the functionalization yield was assumed to be ~67%.

Preparation of Polymer Vesicles Functionalized with Nondendritic Mannose. In order to compare the effectiveness of the dendritic ligand display to the more conventional approach involving the conjugation of individual ligands to the termini of linear polymers, a PBD-PEO derivative with a single terminal mannose group was prepared. First, as shown in Scheme 4, polymer **1** was reacted with a large excess of 4-pentynoic acid to provide the alkyne terminated polymer **10**. This alkyne-terminated polymer was then coupled to (2-azidoethyl)-α-D-mannopyranoside (**11**)[57] to provide polymer **12**. A thin film containing a 50:50 ratio of polymers **1** and **12** was then hydrated to provide vesicle **13** with approximately the same overall density of surface mannose groups as the vesicles functionalized with dendritic mannose described above (Scheme 5). Calculation of the mannose surface density is described in more detail in the Supporting Information. The ability of this polymer mixture to provide well-dispersed, primarily single-walled vesicles was verified by confocal microscopy upon incorporation of the hydrophobic dye Nile Red into the vesicle membrane.

Preparation of Iron Oxide Nanoparticles Functionalized with Dendritic Mannose. In order to further investigate the effect of dendritic surface functionalization on binding to biological targets, iron oxide nanoparticles were also used as a nanoscale platform. These nanoparticles are of significant interest as contrast agents for magnetic resonance imaging and many efforts have been directed toward targeting these agents to specific sites such as tumors and atherosclerotic plaques in vivo using small molecules,[58−60] peptides,[18,19,61] and antibodies.[16,62,63] In most cases, in order to provide water solubility and biocompatibility, these nanoparticles are first functionalized with polymers such as dextran[64] or PEO,[65,66] and then targeting ligands are conjugated to these polymers. Thus, in terms of the binding of ligands to biological targets, these polymer-functionalized nanoparticles would be expected to behave similarly to polymer vesicles or other polymer assemblies.

Analogous to the approach for functionalizing polymer vesicles with dendritic groups, a method for conjugating dendrons to azide functionalized dextran-coated iron oxide nanoparticles was also developed. Thus, nanoparticle **14a** (Scheme 6) having 0.14 μmol of surface azide groups/mg of iron was prepared as previously reported.[67] This nanoparticle was 16 nm in diameter, with a polydispersity of 0.26 as measured by dynamic light scattering, and an iron oxide core diameter of ~5 nm based on transmission electron microscopy. The presence of azide groups on the nanoparticle surface was confirmed by infrared spectroscopy (Figure 4a), and the target quantity of azides on the nanoparticle surface was verified by conjugation of an alkyne-functionalized fluorescent dye (Supporting Information). Next, as shown in Scheme 6, dendron **8** was conjugated to the surface of nanoparticle **14a** in the presence of 9 mM $CuSO_4$ and 30 mM sodium ascorbate in water to provide nanoparticle **15** and the excess dendron was removed by dialysis. Infrared spectroscopy was used to verify completion of the reaction as the peak corresponding to the azide stretch at 2095 cm^{-1} was observed to completely disappear following the reaction (Figure 4c).

Preparation of Iron Oxide Nanoparticles Functionalized with Nondendritic Mannose. To prepare nanoparticles functionalized with nondendritic mannose, 2-isothiocyanato-α-D-mannopyranoside (**4**) was reacted with propargyl amine to provide the alkyne-functionalized mannose derivative **16** (Scheme 6). In addition, nanoparticles **14b** having 0.92 μmol of azide/mg of iron were prepared and characterized as described above. This density of azide groups was chosen in order to obtain approximately the same overall density of mannose on the surface of both the dendritic and nondendritic mannose-functionalized nanoparticles. Thus, **16** was conjugated to nanoparticle **14b** using the same conditions described above for the dendron to provide the nondendritic mannose-functionalized nanoparticle **17**, and the reaction completion was again verified by infrared spectroscopy.

Evaluation of Relative Mannose Binding Affinities. The relative binding affinities of the dendritic and nondendritic mannose functionalized vesicles and nanoparticles were compared using the hemagglutination assay. This assay has been used by several groups to evaluate multivalent displays of mannose.[41,68−71] In the presence of the protein Con A, red blood cells cluster due to interactions of cell surface carbohydrates with the protein. When mannose is present at a sufficiently high concentration, Con A binds preferentially to mannose and the clustering of the blood cells is inhibited. Comparisons of the minimum mannose concentration required to inhibit the agglutination can provide relative binding affinities of mannose-based ligands, which is the main point of interest in this study.

Vesicles **9** and **13** and nanoparticles **15** and **17** were compared with the known ligand α-D-methyl mannopyranoside using this

(57) Chernyak, A.; Gangavaram, S. *Carbohydr. Res.* **1992**, *223*, 303.
(58) Sun, C.; Sze, R.; Zhang, M. *J. Biomed. Mater. Res., Part A* **2006**, *78A*, 550–557.
(59) Weissleder, R.; Kelly, K.; Sun, E. Y.; Shtatland, T.; Josephson, L. *Nat. Biotechnol.* **2005**, *23*, 1418–1423.
(60) Sonvico, F.; Mornet, S.; Vasseur, S.; Dubernet, C.; Jaillard, D.; Degrouard, J.; Hoebeke, J.; Duguet, E.; Colombo, P.; Couvreur, P. *Bioconjugate Chem.* **2005**, *16*, 1181–1188.
(61) Zhang, C.; Jugold, M.; Woenne, E. C.; Lammers, T.; Morgenstern, B.; Mueller, M. M.; Zentgraf, H.; Bock, M.; Eisenhut, M.; Semmler, W.; Kiessling, F. *Cancer Res.* **2007**, *67*, 1555–1562.
(62) Remsen, L. G.; McCormick, C. I.; Roman-Goldstein, S.; Nilaver, G.; Weissleder, R.; Bogdanov, A.; Hellstrom, I.; Kroll, R. A.; Neuwelt, E. A. *Am. J. Neuroradiol.* **1996**, *17*, 411.
(63) Tsourkas, A.; Shinde-Patil, V. R.; Kelly, K. A.; Patel, P.; Wolley, A.; Allport, J. R.; Weissleder, R. *Bioconjugate Chem.* **2005**, *16*, 576–581.
(64) Weissleder, R.; Bogdanoc, A.; Neuwelt, E. A.; Papisov, M. *Adv. Drug Delivery Rev.* **1995**, *16*, 321–334.
(65) Lutz, J. F.; Stiller, S.; Hoth, A.; Kaufner, L.; Pison, U.; Cartier, R. *Biomacromolecules* **2006**, *7*, 3132–3138.
(66) Xie, J.; Xu, C.; Kohler, N.; Hou, Y.; Sun, S. *Adv. Mater.* **2007**, *19*, 3163–3166.
(67) Martin, A. L.; Bernas, L.; Foster, P. F.; Rutt, B. K.; Gillies, E. R. *Bioconjugate Chem,* published online Nov 18, 2008, http://dx.doi.org/10.1021/bc800209u.
(68) Corbell, J. B.; Lundquist, J. J.; Toone, E. J. *Tetrahedron: Asymmetry* **2000**, *11*, 95–111.
(69) Wolfenden, M. L.; Cloninger, M. J. *Bioconjugate Chem.* **2006**, *17*, 958–966.
(70) Kim, B. S.; Hong, D. J.; Bae, J.; Lee, M. *J. Am. Chem. Soc.* **2005**, *127*, 16333–16337.
(71) Dimick, S. M.; Powell, S. C.; McMahon, S. A.; Moothoo, D.; Naismith, J. H.; Toone, E. J. *J. Am. Chem. Soc.* **1999**, *121*, 10286–10296.

Scheme 4

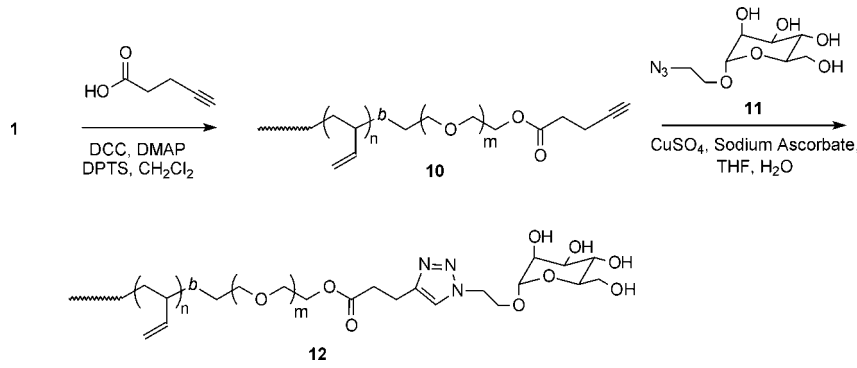

Scheme 5

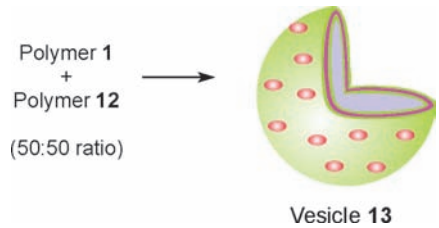

Scheme 6

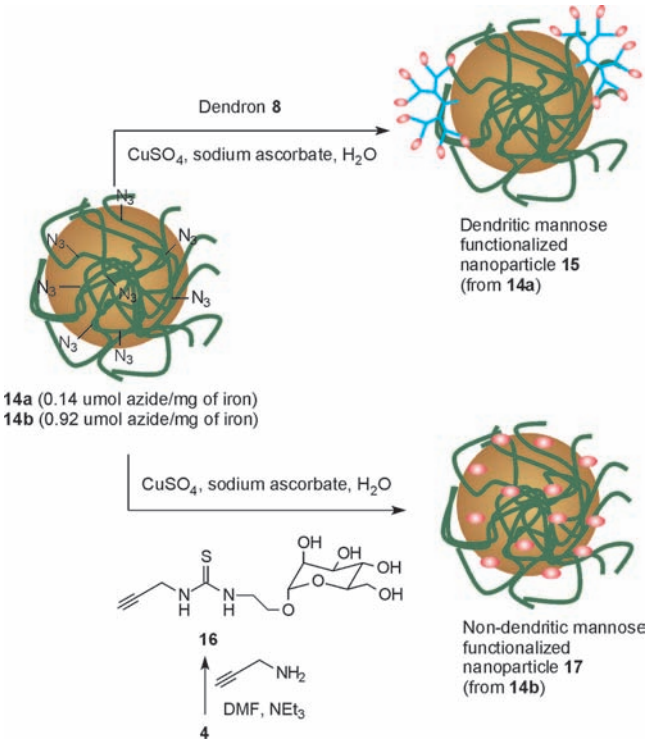

assay. The experiment was carried out at least five times for each system, using blood from different rabbits, on different days, and using different vesicle preparations. By definition, α-D-methyl mannopyranoside was assigned an affinity of 1.0 in this assay, and the relative affinities of the other systems are given in Table 2 on a per mannose basis.

As shown in Table 2, the nondendritic mannose-functionalized vesicle **13** was found to provide only a very modest 3.7-fold increase in affinity despite its multivalency. This enhancement is much less than what was observed by Lee and co-workers previously for mannose-functionalized vesicles;[70]

Table 2. Comparison of the Activities of Dendritic and Nondendritic Mannose-Functionalized Vesicles and Nanoparticles in the Hemagglutination Assay

ligand system	relative activity per mannose
α-D-methyl mannopyranoside	1.0 (by definition)
dendritic mannose-functionalized vesicle **9**	42 ± 27
nondendritic mannose-functionalized vesicle **13**	3.7 ± 1.0
dendritic mannose-functionalized nanoparticle **15**	92 ± 37
nondendritic mannose-functionalized nanoparticle **17**	1.5 ± 0.6

however, their vesicles were formed from relatively rigid, lower-molecular-weight amphiphiles that contained mannose at the end of every oligomer chain. Such vesicles likely have mannose coating the entire surface and are substantially different in properties than most vesicles, including those evaluated here, which are composed of more flexible polymers that inhibit binding more effectively.

In contrast, the dendritic mannose-functionalized vesicle **9** provided a much greater 42-fold increase in relative binding affinity, indicating that dendritic mannose at the vesicle surface can interact much more favorably with Con A. This enhancement is of the same order of magnitude observed previously on a per mannose basis for some multivalent

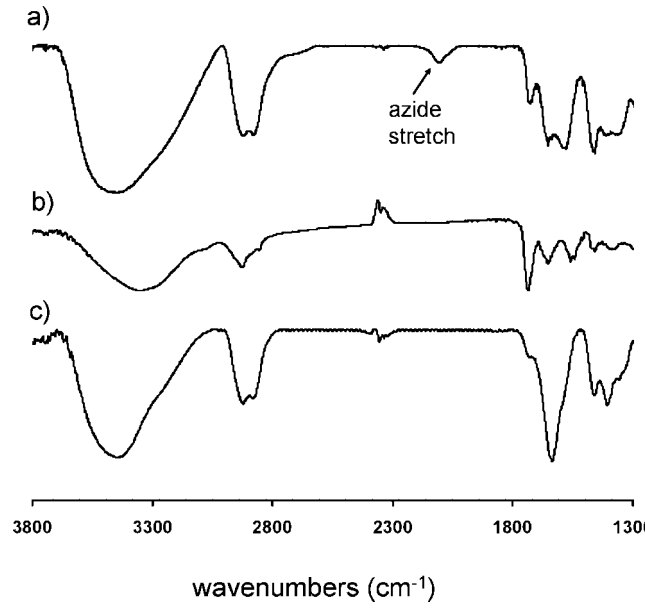

Figure 4. Infrared spectra of (a) nanoparticle **14**, (b) dendron **8**, and (c) nanoparticle **15** demonstrating completion of the conjugation based on disappearance of the azide stretch at 2095 cm^{-1}.

mannose displays.[69,72,73] Although the standard deviation on these measurements is rather high, primarily due to some variability among different blood samples, this is quite common for this assay.[41,74] In addition, as the assay was carried out using serial 2-fold dilutions of the vesicles, the standard deviation represents only approximately ± one dilution in the assay. In every assay, the dendritic mannose-functionalized vesicles inhibited agglutination at lower mannose concentrations than vesicles functionalized with nondendritic mannose. In addition, a *t* test was carried out and the difference in relative binding affinities of the nondendritic and dendritic vesicle systems was found to be statistically significant at the 99.9% confidence level. To investigate whether the variability in results was due to differences in vesicle sizes and polydispersities from preparation to preparation, the assay was also performed with vesicles that were extruded through a 1.0 μm membrane. The resulting vesicles were reproducibly found to be $\sim$1.4 μm in diameter with typical polydispersities of 0.5 based on dynamic light scattering. This led to only small increases in binding affinities and reductions in the standard deviations of the measurements, indicating that vesicle size did not have a major influence on the results of the assay.

Nanoparticle **17** functionalized with nondendritic mannose had essentially no increase in affinity (1.5-fold) relative to methyl mannose, while the dendritic mannose-functionalized nanoparticle **15** exhibited a substantial 92-fold increase in binding affinity on a per mannose basis, an even greater increase than observed for the vesicles. This difference was also found to be statistically significant at the 99.5% confidence level. Dextran-coated iron oxide nanoparticles that were not functionalized with mannose were also evaluated in the hemagglutination assay as dextran is a polymer of glucose and glucose is known to bind con A, albeit more weakly than mannose.[75] No inhibition of agglutination was observed for these nanoparticles, even at very high concentrations.

The enhancement in binding for multivalent ligands has been attributed to several factors. One major factor is commonly referred to as the "chelate effect", which involves both thermodynamic and kinetic components.[33,76] As both the dendritic and nondendritic mannose-functionalized vesicles and nanoparticles can theoretically bind to Con A multivalently due to their large sizes and the presence of multiple mannose molecules on their surfaces, the chelate effect can be considered for each system. Thermodynamically, the binding energy for a multivalent ligand is related to the sum of the enthalpies for each binding event. In general, if the binding of mannose on the surface is hindered by the presence of nearby PEO or dextran, this would make each binding event less favorable. Therefore, the enhanced binding of the dendritic mannose-functionalized materials indicates that the presentation of mannose on dendritic scaffolds is likely an effective means of overcoming steric inhibition by polymers. Due to both the bulky branched architecture of the dendron, as well as possible incompatibilities between the polyester backbone and the hydrophilic PEO or dextran layer, the dendritic mannose may exhibit a greater propensity to be at the surface of the polymer layer in comparison with the nondendritic mannose. Supporting this, it has been previously demonstrated that when biotin is conjugated to a polymer vesicle surface using a polymer chain that is longer than the unfunctionalized polymers in the surrounding membrane, greater adhesion to avidin-coated microspheres was observed.[77] As for the vesicles and nanoparticles functionalized with nondendritic mannose, the biotin groups on polymers of the same length as the surrounding polymers were thought to be buried within the surface PEO brush with little control over the small fraction of biotins extending to the outer surface.[78]

Entropic factors can also be analyzed. In general, the presentation of ligands on relatively rigid rather than flexible scaffolds is more favorable entropically.[33] In the vesicle and nanoparticle systems described here, both the dendritic and nondendritic mannose would be expected to have limited conformational freedom, but the rather rigid and sterically hindered display of mannose on the dendritic scaffold provides a small entropic advantage. All of the above factors, which can affect the thermodynamics of binding would also be expected to kinetically accelerate the binding of the dendritic versus nondendritic mannose-functionalized materials, which would be particularly important in a dynamic situation such as in flowing blood in vivo. Kinetics cannot be ruled out as playing a role in the hemagglutination assay; however, it is unlikely that they were the major factor as the rate of binding between multivalent mannose displays and Con A has been reported to be quite fast ($k_{on} \cong 10^5$ min^{-1}), and the vesicles or nanoparticles were incubated with Con A for 2−3 h before the addition of red blood cells.[40]

Another aspect of multivalent ligands that has been proposed to be important is a "statistical" or "proximity" effect that is associated with highly localized concentrations of a ligand.[69] This effect has been proposed to partly explain the enhanced binding of multivalent ligands that cannot span the distance between receptor binding sites and cannot benefit from the chelate effect described above. In the case of Con A, the distance between binding sites is $\sim$6.5 nm.[79] While both the dendritic and nondendritic mannose-functionalized vesicles and nanoparticles can undergo multivalent binding, the dendron with an estimated maximum distance between mannose groups of 3−4 nm is not large enough that multiple mannose groups on the same dendron can undergo simultaneous binding to multiple sites on Con A. Overall, both the dendritic and nondendritic systems were designed to display the same density of mannose on their surfaces; however, the more localized "clusters" of mannose presented in the dendritic systems provide advantages via the "proximity" effect. Similarly, it has previously been shown that tetraantennary mannosyl conjugates displayed at the surfaces of liposomes provided enhanced binding to Con A relative to their monomannosyl analogues.[72] This was attributed to the organization of mannose into clusters as there were no polymer chains to provide steric inhibition in that case.

Another explanation that has been proposed to explain the binding of small carbohydrate clusters is their ability to induce

(72) Espuelas, S.; Haller, P.; Schuber, F.; Frisch, B. *Bioorg. Med. Chem. Lett.* **2003**, *13*, 2557–2560.
(73) Lin, C. C.; Yeh, Y. C.; Yang, C. Y.; Chen, G. F.; Chen, Y. C.; Wu, Y. C.; Chen, C. C. *Chem. Commun.* **2003**, 2920–2921.
(74) Wolfenden, M. L.; Cloninger, M. J. *J. Am. Chem. Soc.* **2005**, *127*, 12168–12169.
(75) Schwarz, F. P.; Puri, K. D.; Bhat, R. G.; Surolia, A. J. *J. Biol. Chem.* **1993**, *268*, 7668–7677.
(76) Lundquist, J. J.; Toone, E. J. *Chem. Rev.* **2002**, *102*, 555–578.
(77) Lin, J. J.; Silas, J. A.; Bermudez, H.; Milam, V. T.; Bates, F. S.; Hammer, D. A. *Langmuir* **2004**, *20*, 5493–5500.
(78) Dan, N.; Tirrell, M. *Macromolecules* **1993**, *26*, 6467–6473.
(79) Naismith, J. H.; Emmerich, C.; Habash, J.; Harrop, S. J.; Helliwell, J. R.; Hunter, W. N.; Raferty, J.; Kalb (Gilboa) , A. J.; Yariv, J *Acta Crystallogr., Sect. D: Biol. Crystallogr.* **1994**, *50*, 847–858.

the formation of soluble or insoluble aggregates of lectins such as Con A, in an entropically driven process.[76] In order for the dendritic system to provide an advantage over the nondendritic system here, it is necessary for a single dendron on the surface to simultaneously bind to more than one molecule of Con A. This is unlikely due to the relatively small size of the dendron and the resulting steric effects at the surface. Finally, it has been proposed that large multivalent systems such as macromolecules may provide enhanced binding relative to monovalent mannose in assays such as the hemagglutination assay due to their abilities to provide steric stabilization which prevents the binding of Con A to additional ligands. Vesicles and nanoparticles can provide effective steric stabilization such that following the binding of Con A to the vesicle or nanoparticle surface it is less likely that another ligand on the surface of a red blood cell can bind to another site on Con A. Nevertheless, this would not explain differences between the dendritic and nondendritic systems. Therefore, the enhancement in binding of the dendritic mannose-functionalized systems can be attributed mainly to the dendron's ability to effectively display mannose at the surfaces of the materials, overcoming steric inhibition by surrounding surface polymer chains, as well as the presentation of mannose in highly localized clusters.

Conclusions

The goal of this study was to evaluate whether the way in which biological ligands are presented at the surfaces of nanomaterials would affect their binding to biological targets. To this end, polymer vesicles and dextran-coated iron oxide nanoparticles were successfully functionalized with both dendritic and nondendritic displays of mannose, a well-known multivalent ligand, and their binding affinities were compared using the hemagglutination assay. It was found that for both vesicles and nanoparticles the binding of the dendritic mannose-functionalized materials was enhanced by 1−2 orders of magnitude relative to the nondendritic system. This can be attributed to the enhanced availability of the dendritic molecules on the surface due to their lower susceptibility to becoming buried within the polymer coating. In addition, the localized clusters of ligands presented in the case of the dendritic systems can enhance binding due to localized high concentrations or a "proximity effect". This result is important as there is significant interest in controlling the biological behavior and targeting of materials with capabilities for delivering drugs and imaging agents to medical targets. As this result has been demonstrated to apply to materials as diverse as polymer vesicles with a PEO surface block and dextran-coated iron nanoparticles, it should also hold for a wide range of other polymer assemblies and polymer-coated inorganic nanoparticles. Thus, this study reveals that the binding affinity of biological ligands presented at polymer surfaces can be significantly enhanced using dendritic scaffolds.

Acknowledgment. We thank the Government of Ontario (Ontario Graduate Scholarship in Science and Technology to ALM), the Natural Sciences and Engineering Council of Canada (NSERC), the Canada Research Chairs program, and the University of Western Ontario for funding this research.

Supporting Information Available: Details of all chemical syntheses, vesicle and nanoparticle preparations, confocal laser scanning miscroscopy, UV−visible spectroscopy, nanoparticle characterization, hemagglutination assay, and NMR spectra of all new molecules. This material is available free of charge via the Internet at http://pubs.acs.org.

JA807220U